Li et al. Journal of Infrastructure Preservation and Resilience (2021) 2:14
https://doi.org/10.1186/s43065-021-00029-y

Journal of Infrastructure Preservation and Resilience

RESEARCH Open Access

2D-wavelet based micro and macro texture analysis for asphalt pavement under snow or ice condition

Feng Li[1], Gulnigar Ablat[1], Siqi Zhou[1*], Yixin Liu[1], Yufeng Bi[2], Zihang Weng[3] and Yuchuan Du[3]

Abstract

In ice and snow weather, the surface texture characteristics of asphalt pavement change, which will significantly affect the skid resistance performance of asphalt pavement. In this study, five asphalt mixture types of AC-5, AC-13, AC-16, SMA-13, SMA-16 were prepared under three conditions of the original state, ice and snow. In this paper, a 2D-wavelet transform approach is proposed to characterize the micro and macro texture of pavement. The Normalized Energy (NE) is proposed to describe the pavement texture quantitatively. Compared with the mean texture depth (MTD), NE has the advantages of full coverage, full automation and wide analytical scale. The results show that snow increases the micro-scale texture because of its fluffiness, while the formation of the ice sheets on the surface reduces the micro-scale texture. The filling effect of snow and ice reduces the macro-scale texture of the pavement surface. In a follow-up study, the 2D-wavelet transform approach can be applied to improve the intelligent driving braking system, which can provide pavement texture information for the safe braking strategy of driverless vehicles.

Keywords: 2D-wavelet, Asphalt pavement, Micro-texture, Macro-texture, Ice, Snow

Introduction

The pavement texture refers to the characteristics of the concave-convex structure on the surface areas, and it is an important index to evaluate the roughness of the pavement surface. The pavement surface texture was subdivided into four ranges based on the wavelength by PIARC [19]: microtexture, macrotexture, megatexture, and unevenness with wavelengths from 0 mm to 0.5 mm, 0.5 mm to 50 mm, 50 mm to 500 mm and 500 mm to 50 m, respectively. It is known from the reports by various studies that the pavement surface texture plays a significant role in the road skid resistance performance. These texture scales have different contributions to tire-pavement friction [14]. Typically, a more pronounced depth of macrotexture leads to a better skid resistance performance for roads of the same material [23, 24].

Snow and ice weather have a significant influence on the skid resistance of pavement. In snow and ice weather, the ice or snow attached to the pavement surface will fill the gap of the mixture, significantly reduce the roughness of the pavement surface texture, and significantly change the skid resistance performance of the road surface, which could lead to treacherous driving conditions (Huaxin [12, 17, 28]).

Pavement surface texture is usually characterized by the mean texture depth (MTD) and the mean profile depth (MPD). Previous research shows that the two parameters are highly correlated [20]. On the one hand, the mean texture depth (MTD) obtained by the sand patch method is not accurate enough to ensure the objectivity of the testing results. On the other hand, the mean profile depth (MPD) by high-speed profiler measurements do not consider all surface profile properties. From what has been discussed above, the two description methods cover many original features of pavement

* Correspondence: zsq47@buaa.edu.cn
[1]School of Transportation Science and Engineering, Beihang University, Beijing 100191, China
Full list of author information is available at the end of the article

surface texture and fails to meet the needs of current research.

In recent years, various methods have emerged to characteristics of pavement macrotexture accurately [15, 21, 22]. High-resolution equipments are frequently used to obtain three-dimensional texture information of road surface ([25, 26, 31]). Mistakidis used the surface fractal dimension to describe the pavement texture [16]. De Chen proposed a cost-effective and relatively precise image-based texture analysis method (ITAM) based on digital image processing and spectral analysis technologies [7, 8]. Puzzo Lorenzo used five common cameras to collect pavement surface pictures and calculate the digital Mean Texture Depth (MTD) starting from the Digital Surface Model (DSM) generated by the photos [20]. Liqun Hu used a handy laser scanner to collect 3D texture data of asphalt surface, and eight different roughness parameters were used to describe the 3D characteristics of macrotexture images [11]. Persson presented a mathematical model that quantitatively determines the kinetic friction coefficient of rubber sliding against a hard, rough substrate, which can be used to predict and calculate skid resistance [18]. Andreas Ueckermann used a chromatic white light sensor to measure pavement texture and calculated the skid resistance based on the measured texture by means of a rubber friction model [3].

Signal processing methods were applied to analyze the texture data through the researchers' study in recent years [10]. Aggregate physical descriptors and Fourier transforms have been used to characterize the texture properties of the aggregates used in asphalt concrete surface courses [6]. The power spectral density (PSD) was applied to analyze the pavement texture profile signals [1]. However, the advanced data analysis methodologies mask the spatial reference of the data [13]. Wavelet transforms allow frequency domain analysis while preserving spatial reference [4]. Hence, the wavelet transform was carried out to research the correlation between MPD and wavelet-based parameters [27, 29, 30]. The wavelet analysis was applied in quantifying aggregate particle surface texture using two-dimensional (2D) grey-scale images [2]. Work by Abbas et al. also used wavelet analysis to characterize the 3D surface texture of Portland cement concrete (PCC) cores captured through X-ray computed tomography [1]. Yuchuan Du conducted the 2D-wavelet decomposition on eight types of mixtures and used the Relative Energy (RE) and 2D-Entropy to represent the mixture surface texture distribution properties [9].

After making a general survey of studies conducted in the past decades, there is still an obvious limitation that the previous research only focuses on the profile analysis in one direction and neglects the entire surface feature. The pavement surface is a complex three-dimensional structure, and many important features will be lost in transforming the three-dimensional pavement surface structure into two-dimensional images and sections. Therefore, the current indicators are the average value of calculating the feature based on a two-dimensional profile, so they lack spatial relations and cannot accurately represent the pavement texture. Because of the above shortcomings, this paper analyzes the three-dimensional pavement surface structure.

This paper aims to implement a two-dimensional discrete wavelet transform to decompose pavement surface texture at micro and macro scales. The 2-D wavelet transform approach separates microtexture and macrotexture into six levels by wavelengths while preserving spatial information. The total energy of each level and the normalized energy (NE) of all surface macro-scale textures are used as the wavelet-based indicators. To evaluate the pavement texture performance under ice or snow condition, we compare the decomposition results of five types of mixtures under three different conditions.

Table 1 compares the methods used to characterize the micro and macro texture of pavement in this paper with those used in other researches.

Data acquisition and processing

Preparation of test specimens

In this paper, two types of asphalt mixtures (asphalt concrete (AC), stone mastic asphalt (SMA)) were chosen to characterize the pavement texture. Three nominal maximum aggregate sizes (NMAS) were used with mixture AC (AC-5, AC-13, AC-16). At the same time, two NMASs were used with SMA (SMA-13, SMA-16). The forming method of the mixture specimen was the wheel - grind method. Figure 1 shows the grading curve of the mixture types.

The asphalt mixture slabs of different gradation types were respectively cut into three specimens of 100 mm × 300 mm × 50 mm. A simulated test of snow and ice on the five mixtures surface was carried out to describe the influence of snow and ice on the surface texture. When simulating the road surface with ice, water was sprinkled on the surface of the specimens and frozen outdoors at − 10 °C for 1 h. Considering the rolling action of the wheel on the road surface, the snow was scattered on the surface of the specimens and compacted with a rubber hammer to simulate the texture state of the pavement surface after snow.

Data acquisition

In order to measure the surface texture of the specimen, we used a high-resolution three-dimensional profile scanner called VR-3000, which is developed by the company KEYENCE. In this paper, the scanning rate was set to 12x. The scanning accuracy of the apparatus is 1 μm for horizontal and 0.5 μm for vertical, the sampling

Table 1 Review of pavement texture research methods

Method/Equipment	Description	Measuring parameters	Characteristics
Sand patch method	Spread sand with a volume of 25 cm^3 on the measuring point to form a uniform circle and measure the diameter of the circle. The result is the volume of the sand divided by the spread area.	Mean Texture Depth (MTD)	The method is simple but with large error, and is not suitable for large sample detection.
The 1-kHz laser scanner	The scanner is capable of measuring texture with wavelength as low as 0.03 mm.	Mean Profile Depth (MPD), Root Mean Square (RMS)	This equipment can be used to evaluate both macro and micro textures. Besides, it allows users to produce repeatable texture parameters and to capture the detailed surface features.
HandySCAN 300	The device provides resolutions as clear as 0.100 mm, and precision as high as 0.040 mm.	The coordinates of the 3D data of surface point cloud	High adaptability, high precision, after obtaining the point cloud data, the 3D model can be reconstructed by software.
Close range (stereoscopic) photogrammetry or microscopic measurement	Based on images captured by a camera or microscope, proprietary software is used to model and analyze them in three dimensions.	Mean Texture Depth (MTD), spectral indicators	the visualization of 3D terrain, Overlay micro texture, macro texture and coarse texture.
VR-3000 (this paper)	This paper aims to implement a two-dimensional discrete wavelet transform to decompose pavement surface texture at micro and macro scales.	Mean Texture Depth (MTD), Normalized Energy (NE)	Compared with MTD values, the NE values have the advantages of full coverage, full automation and wide analytical scale.

frequency of the specimen scanning in this paper is 1 mm. The scanner measured the surface texture of a 200 mm × 100 mm area at one time. After the scanning, the texture data was cropped to the size of 110 mm × 80 mm according to the marked points on the specimen in advance to ensure the same position of each measurement every time. Three-dimensional scanning results of the specimen surface are shown in Fig. 2. The bright colored areas, such as red, can be regarded as the convex parts of the specimens, while the dark colored areas, such as blue, can be regarded as the concave parts of the specimens.

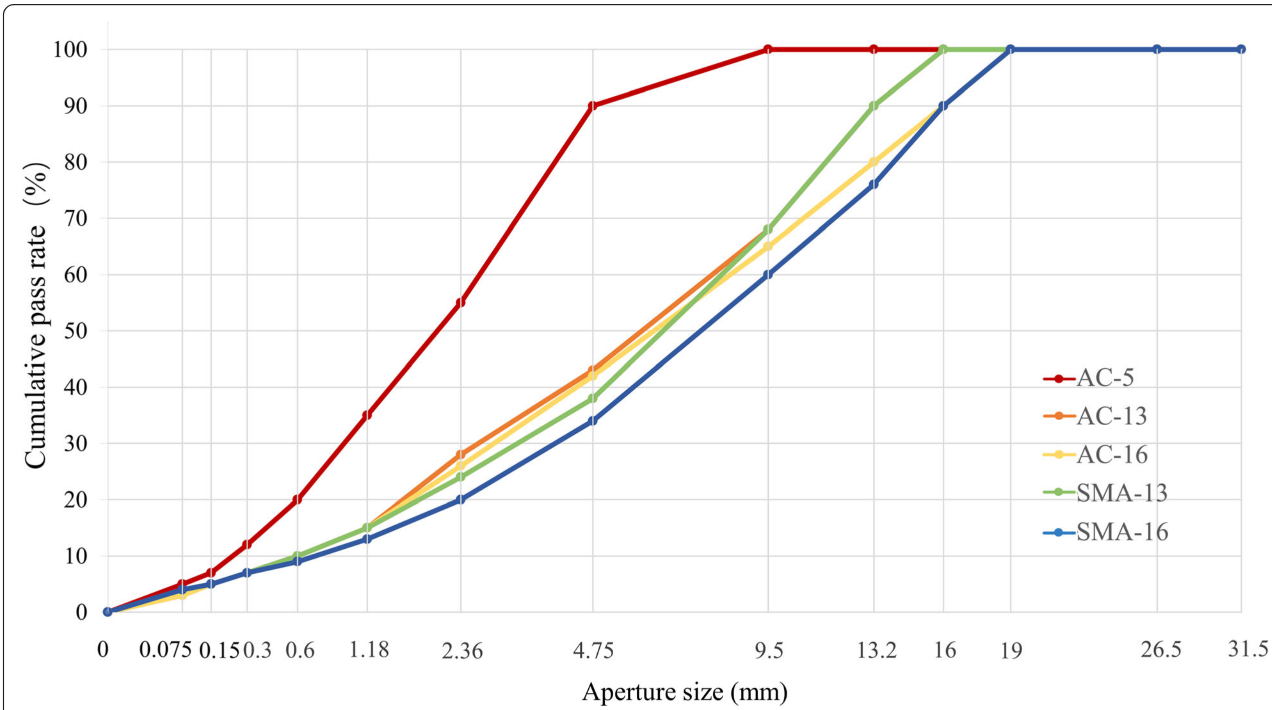

Fig. 1 Grading Curve

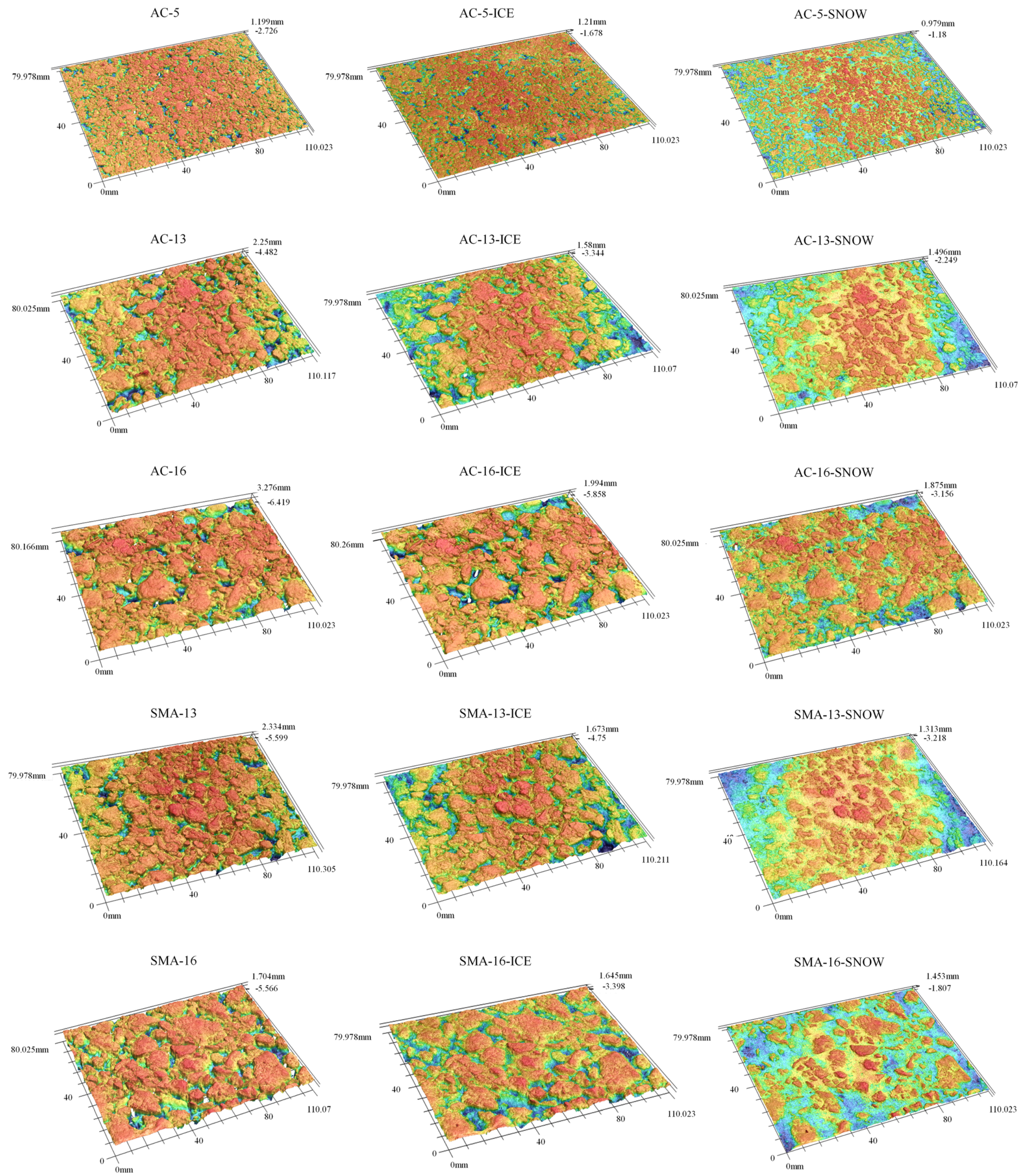

Fig. 2 Three-dimensional scanning results of the specimen surface

After getting the scanned data, it is necessary to pre-process the data first. The first step was meshing the point cloud. A 1170 × 850 grid was established at 0.1 mm intervals both in x- and y-direction. The interpolation method was applied to assign values to z in the grid. Afterward, the data were normalised by subtracting the mean value. However, because of the roughness of the pavement texture, the scanner will miss some concave data blocked by the convex texture. In order to ensure the accuracy of the data, we need to use a 2-D filter to remove the outliers in the scanned data. A 3*3 sliding window was applied to detecting outliers in two directions with a step size of 1. When the variance of z (z means the height of the point) of the points in the sliding window was greater than a certain threshold (0.1 in this paper), the point was regarded to be abnormal, and its value was replaced by the median value of the surrounding points.

Considering that the contact part of the tire and road surface where friction occurs is located at the top of the road surface, the roughness of the top topographic surface of the road surface is characterized in this study. The skid resistance performance of the asphalt mixture is closely related to its surface convex and concave distribution, which is a macroscopic reflection of its microstructure [5]. The convex points are the main factors of hysteresis on dry roads, and the concave points are the main factors of drain away running water on wet roads, so the concave and convex points are necessary conditions for skid resistance. In this paper, the influence of convex points on skid resistance performance is mainly considered, but the influence of concave points on drainage is not considered. Kanafi and Tuononen suggest that the analysis from a top cut of the surface topography on 50% or less surface area and found a high correlation with friction and top 20% of PSDs [13]. The top PSD calculated at any portion of the top surface profile except the top 50% leads to false conclusions about the actual asperity distributions. In this paper, based on existing practical experience, the top 50% of the fractal surface was selected as the cutting plane for research and analysis and the top 100% of the fractal surface was used to make comparative observations, and the z values below the plane were denoted as zero. Figure 3 shows the fractal surface plane on the different cutting planes.

Extended measuring method of MTD

There are many standard parameters for the characterization of the pavement surface macrotexture. The most commonly used parameters are mean texture depth (MTD), mean profile depth (MPD), and sensor measured texture depth (SMTD). Among them, MTD is obtained by calculating the ratio of the volume of sand to the average area of the covered circle by the sand patch method. Although this method is easy to operate and has no special requirements for operators, reproducing the results on one spot is difficult so that it is not suitable for large-sample testing. At the same time, this method is a fixed-point detection method, which cannot reflect the macrotexture of the whole region. After the surface profile is generated by the laser detection system, MPD and SMTD can be calculated according to the average algorithm, which can be used to represent the construction depth of the landmark. However, they have similar limitations to MTD. For example, the use of average algorithms masks some of the macroscopic construction characteristics of the pavement surface.

In this study, based on the basic MTD measurement principle that the ratio of the volume of sand and the area of the sand, an extended method of MTD is proposed. The concave volume can be easily obtained from the software VR-3000, which is the bundled software with the 3D scanner. As shown in Fig. 4, after setting the peak and nadir plane, the volume of the blue area means the concave diagram. The area of the texture is the scanning area. The MTD is calculated by the following equation:

$$MTD = \frac{V_c}{S} \tag{1}$$

where V_c is the concave volume, and S is the scanning area.

Wavelet transform

As we all know, the wavelet transform is an improved method of Fourier transform, which is widely used for multi-scale signal decomposition. Mallat came up with an efficient algorithm for discrete wavelet transform which is widely used in pavement texture analysis [27, 29, 30].

In Mallat's algorithm, the wavelet transform decomposes the discrete signal s into an equivalent

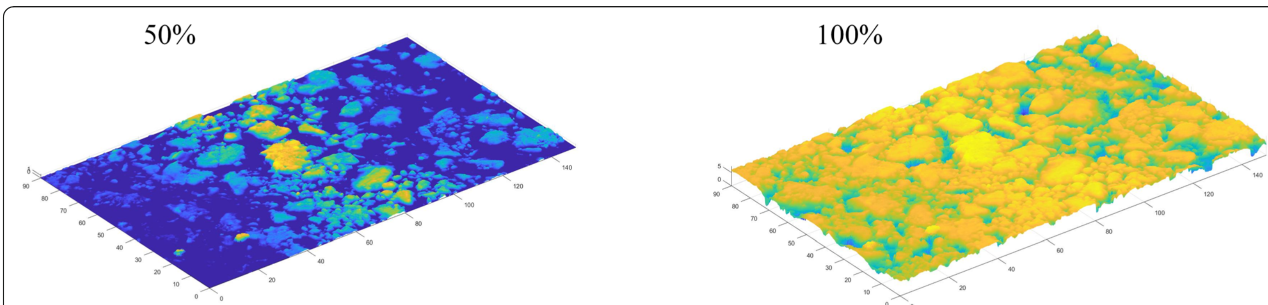

Fig. 3 An Example of Fractal Surface on Different Cutting Plane

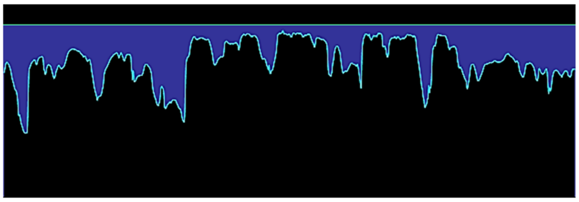

Fig. 4 Concave volume diagram

approximation signal and a detail signal. The approximation signal is subsequently decomposed into another set of approximation and detailed signals and so on (i.e. the approximate component a_i is decomposed into a_{i+1} and d_{i+1}).

For signal s, the wavelet transform decomposition process of five-level can be represented by

$$\begin{gathered} s = a_1 + d_1 \\ s = a_2 + d_2 + d_1 \\ s = a_3 + d_3 + d_2 + d_1 \\ s = a_4 + d_4 + d_3 + d_2 + d_1 \\ s = a_5 + d_5 + d_4 + d_3 + d_2 + d_1 \end{gathered} \tag{2}$$

The energy is an indicator that measures the overall condition of each part. Two-dimensional wavelet energy can be denoted as:

$$E = \sum_x \sum_y \left| Z_{x,y} \right|^2 \tag{3}$$

The unit of wavelet energy is the square of the unit of length (e.g., mm2), which represents the sum of squares of the elevation of the macro texture profile. The energy (E) characterizes the overall roughness, which varies significantly from different specimens. Moreover, for the same specimen, E is susceptible to slight changes in the detection position. Therefore, the Relative Energy (RE) is considered to represent the proportion of energy of each scale in the total energy, is introduced as:

$$RE_{ij} = \frac{E_{ij}}{\sum_{i=1}^{n} \sum_{j=1}^{n} E_{ij}}, \quad (1 \le i \le n, 1 \le j \le n) \tag{4}$$

where E_{ij} represents the energy of wavelet band decomposed in two directions.

The Normalized Energy (NE) allows comparisons between total energy statistics obtained from different specimens.

$$NE = \frac{\sum_{i=1}^{n} \sum_{j=1}^{n} E_{ij}}{Ndxdy} \tag{5}$$

where dx is the sampling interval in the x-direction (e.g., m), dy is the sampling interval in the y-direction (e.g., m). N is the number of points that are calculated.

In this paper, the analysis was carried out using MATLAB Wavelet Toolbox. The selection of the mother wavelet function plays a critical role in the wavelet transform. The Daubechies wavelet families are the most common application in surface texture analysis, which is composed of 10 compactly supported orthonormal wavelet functions (db1, db2, db3, …, db10). Several studies have used db3 mother wavelet to analyze pavement surface texture, roughness, and degree of aggregate segregation. The Symlets wavelets are the improved version of dbN. In this paper, sym4 was chosen as the mother wavelet for further analysis.

Decomposing the data into six levels, five of which were the detail signal denote as Level 1 (d1), Level 2 (d2), …, Level 5 (d5). Level 6 (a5) represents the approximation signal. The wavelengths of the decomposition levels are 0.1881 mm, 0.3761 mm, 0.7523 mm, 1.5046 mm, 3.0092 mm, 6.0183 mm. According to the definition specification, the wavelength range of macrotexture is 0.5 mm ~ 50 mm. Therefore, Level 3 ~ Level 6 represents macro-texture. Two-dimensional discrete wavelet transform algorithm is used by decomposing the data in both x- and y-direction, as shown in Fig. 5.

Results and discussion

Determination of MTD

A comparison between the original specimens and the ice-snow conditions, specimens MTD results is shown in Fig. 6. The higher the MTD value, the more complex the macrotexture of the road and the rougher the surface.

The texture complexities of different specimens were analyzed by comparing the MTD values of the original surfaces of the five specimens in Fig. 6. A closer look at the statistic reveals that higher MTD values were measured in SMA specimens, which means SMA is rougher than AC. Compared with all the specimens, AC-5 had the lowest MTD values and SMA-13 had the highest MTD values. As can be noticed from Fig. 1, the SMA specimens used a gap grinding, which considered a higher percentage of coarse aggregates resulting in higher MTD results. AC-5 had the lowest MTD values because of its minimum nominal particle size. Normally, SMA-16 should have the highest MTD values; however, because the feature extraction area of the scanner was small, the texture features of SMA-16 specimens with larger aggregate size were not fully displayed in a small area, so the experimental results showed that SMA-13 had the highest MTD values.

The detailed statistical analysis was asked to identify the changes of MTD values when specimens were in ice or snow conditions. It can be noticed from Fig. 6 that, for most different types of asphalt mixtures, the original surface had the highest MTD value when the surface with snow had the lowest MTD value. The reason why AC-5 had different results from others is when sprayed

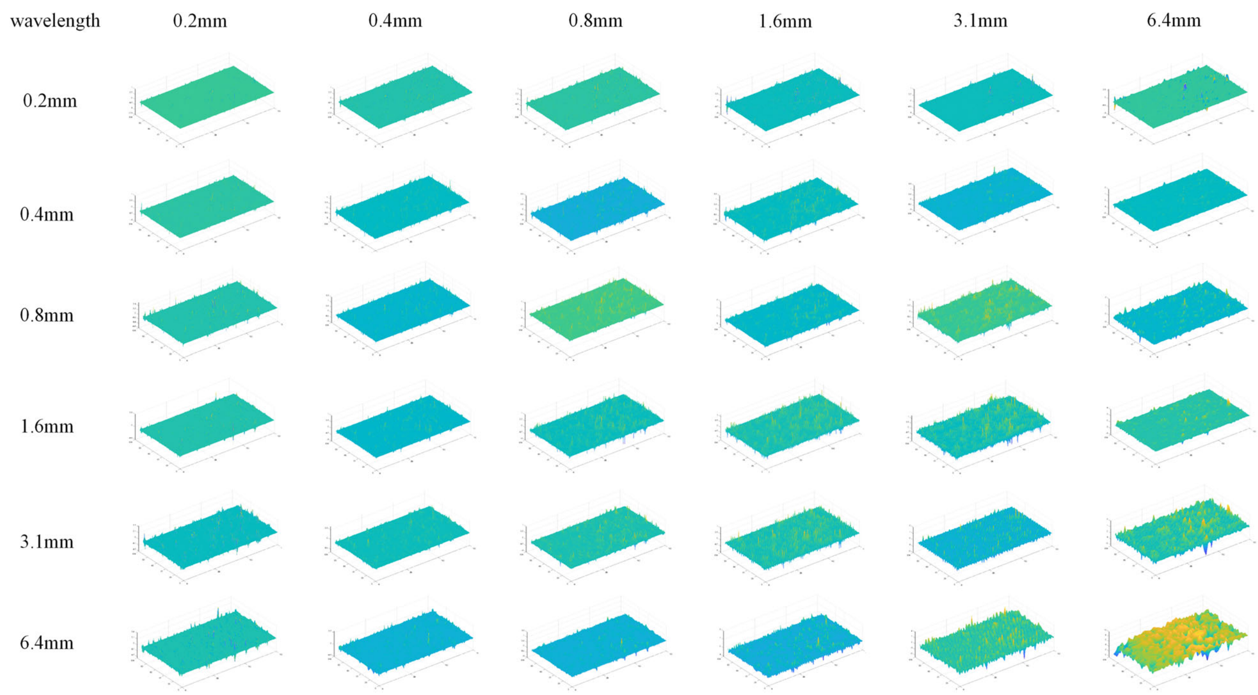

Fig. 5 Two-dimensional discrete wavelet transform

water on the surface, AC-5 formed an ice sheet on the surface because of its dense structure. At the same time, water sprayed on other specimens permeated into the texture slot and frozen. In general, the MTD value range from 0.469 mm for the frozen AC-5 specimen surface to 1.741 mm for the original SMA-13 surface.

Determination of wavelet energy

The 2D energy matrix was formed as 6*6. The levels in two dimensions are redefined in Fig. 5: Level 6 includes the sixth row and column; Level 5 contains the fifth row and column except for the part in Level 6; Level 4 includes the fourth row and column except for the part in Level 5 and 6, and so on. As mentioned above, the 3-D model was respectively cut at the top 50% and 100% of a fractal surface plane. Figures 7,8, 9, 10 and 11 show the energy results on the 50% and 100% cutting plane in micro- and macro-scale. In each of the figures below, the black line represents the original surface, the red line represents the icy surface, and the blue line represents the snowy surface.

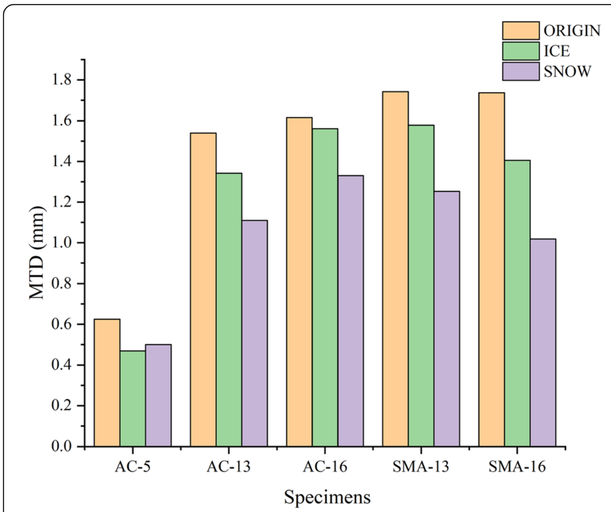

Fig. 6 MTD Results

The wavelet energy parameter for each of the decomposition levels can be used to explain the differences in the properties of pavement surfaces. It can be seen from Figs. 7,8, 9, 10 and 11 that the micro-scale energy results of AC-5, SMA-13, SMA-16 specimens on the 50% cutting plane were consistent. On the micro-scale, the original surface showed the highest energy and the icy surface showed the lowest energy. As for the micro-scale energy results of AC-13 specimens, the energy results of icy surface and snow surface were quite similar; the factors that contribute to this situation include the errors generated in the preparation and data collection of specimens. In the micro-scale energy results of AC-16 specimens, the energy value of the snowy surface exceeded that of the original surface. The above characteristics showed that snow increases the micro-scale texture of the pavement surface because of its fluffiness, which leads to severe irregularities on the micro-scale, and the

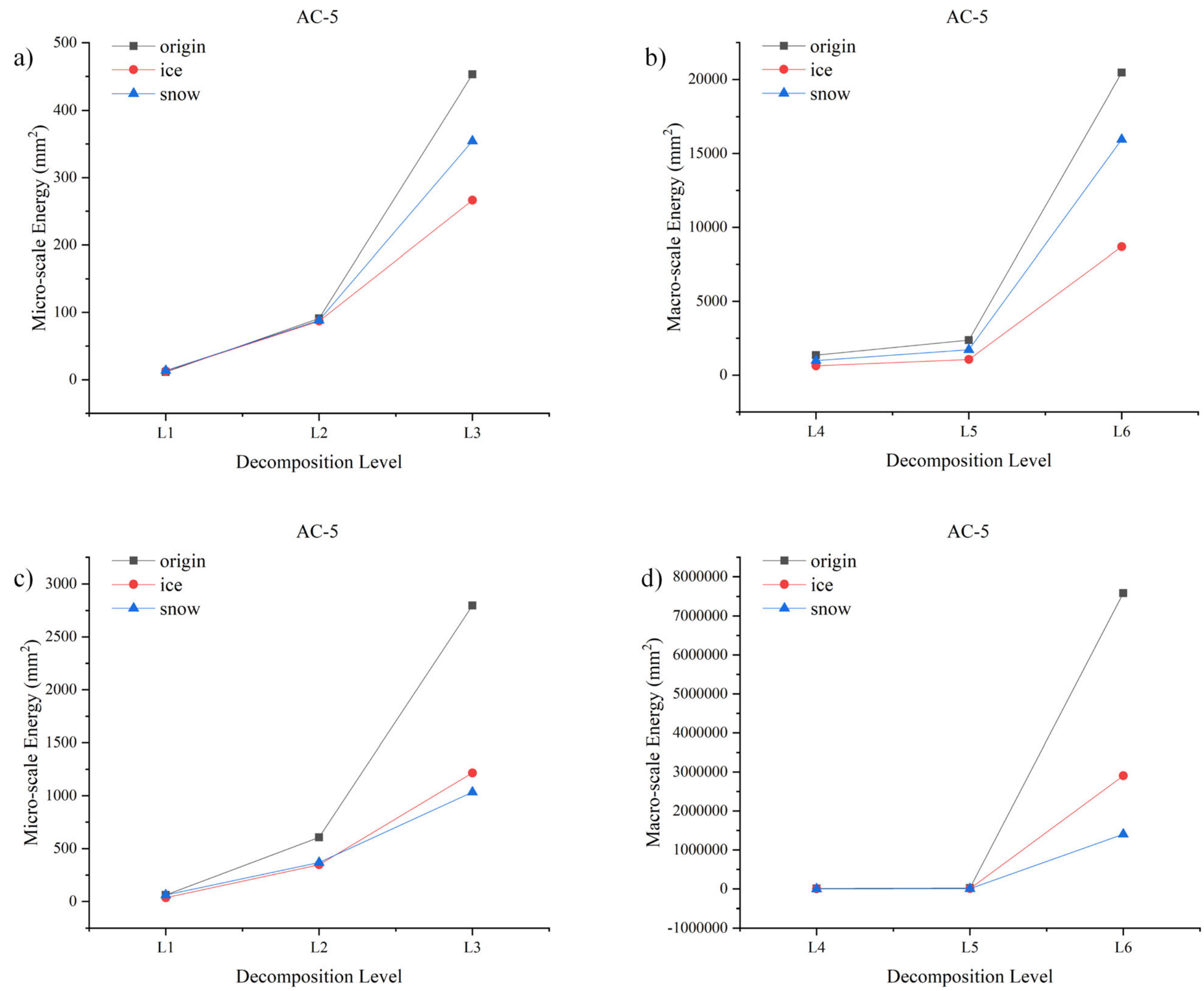

Fig. 7 The Energy Results of AC-5; **a** 50% Cutting Plane in micro-scale, **b** 50% Cutting Plane in macro-scale, **c** 100% Cutting Plane in micro-scale, **d** 100% Cutting Plane in macro-scale

snow surface has abundant micro-scale texture. The icy surface had the lowest energy and the simplest micro-scale texture, which meant the formation of ice sheets on the surface reduced the micro-scale texture.

In Figs. 8, 9, 10 and 11, it is shown that the macro-scale energy results of AC-13, AC-16, SMA-13 and SMA-16 specimens on the 50% cutting plane are consistent. The original surface showed the highest energy and the snowy surface showed the lowest energy. It indicated that the original surface texture is the most complex, and because of the filling effect of snow and ice on the surface texture, the energy value of the pavement surface was reduced.

In Figs. 7,8, 9, 10 and 11, it can be seen that the energy results of each mixture type on the 100% cutting plane showed the same change rule no matter on the macro scale or the micro-scale. The original surface showed the highest energy and the snowy surface showed the lowest energy.

Wavelet NE results

The energy on a single scale is not suitable to represent the overall macrotexture of the pavement surface. Therefore, the Normalized Energy (NE) was proposed as a new alternative metric to characterize the overall pavement macrotexture. NE is introduced as Eq. (7). This statistic represents the sum of the squares of the profile for the wavelengths in the macrotexture range. For the data set analyzed in this paper, it includes wavelengths longer than 0.5 mm (i.e., wavebands d_4 to d_6).

Figure 12 presents a comparison of wavelet NE values of the selected pavement specimens under various

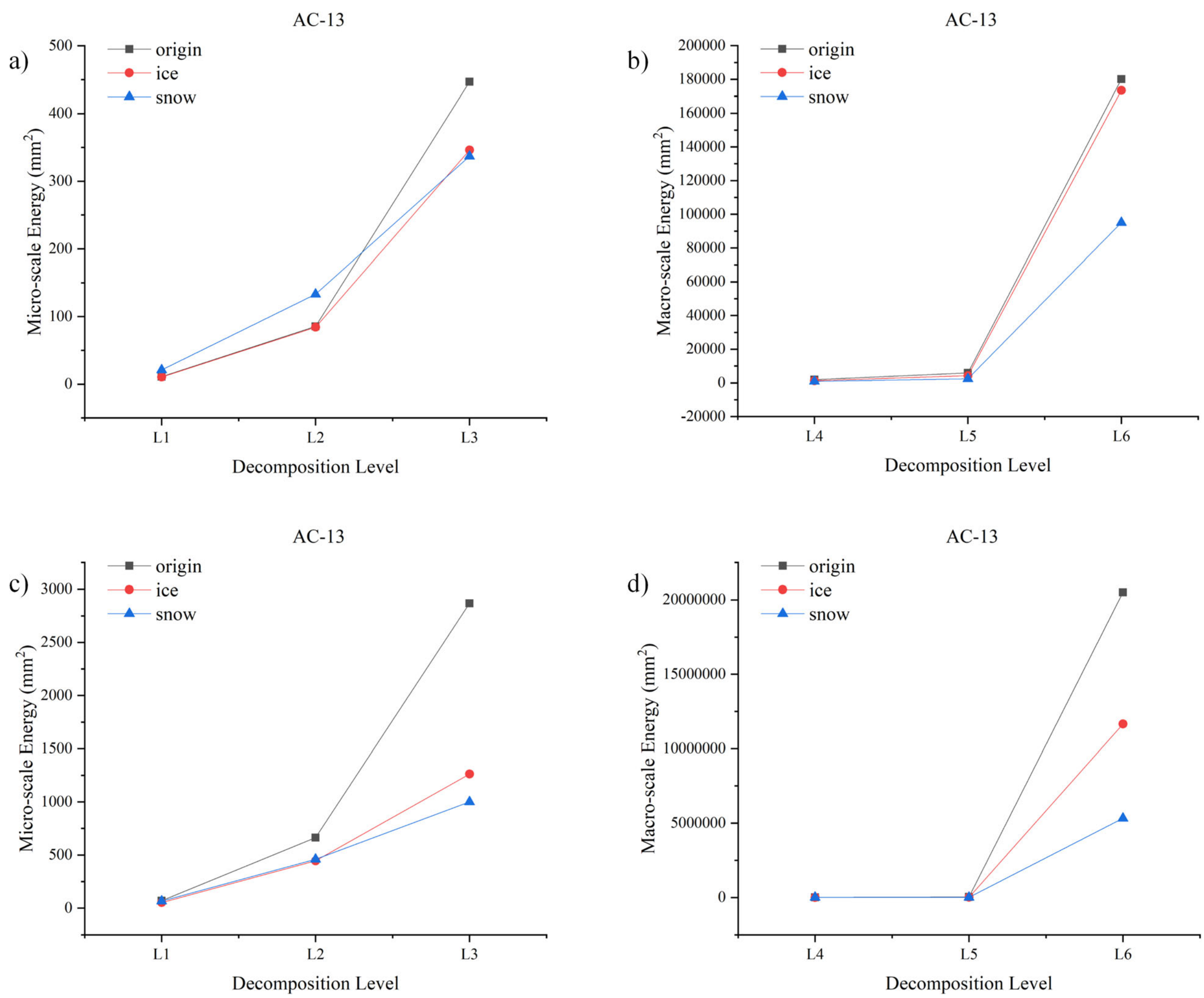

Fig. 8 The Energy Results of AC-13; **a** 50% Cutting Plane in micro-scale, **b** 50% Cutting Plane in macro-scale, **c** 100% Cutting Plane in micro-scale, **d** 100% Cutting Plane in macro-scale

conditions. A Higher NE value indicates more complex macrotexture and vice versa. Firstly, the NE values of the original surfaces of various specimens were compared and analyzed. As shown in Fig. 12, on the 50% cutting plane, the maximum value of NE is 26.785 measured by the SMA-13 specimen, and the minimum value of NE is 2.810 measured by the AC-5 specimen. As can be noticed from Fig. 1, the SMA specimens used a gap grinding, which considered a higher percentage of coarse aggregates resulting in higher NE results. It is an unexpected result that SMA-16, which has a larger aggregate particle size, has a lower NE value than SMA-13, so as the AC-13 and AC-16. The reason for this result may be due to the limited scanning area of the 3D profile scanner, that larger particle size reduces the macrotexture of the surface. The NE results on the 50% cutting plane are consistent with the MTD results of the original surfaces of various specimens mentioned above. On the whole, the NE value of the AC mixture type was less than that of the SMA mixture type. While the results of the 100% cutting plane of each gradation type show different characteristics from that of the 50% cutting plane. On the 100% cutting plane, the maximum value of NE is 4721.311 measured by the AC-16 specimen and the minimum value of NE is 865.374 measured by the AC-5 specimen. It shows that the texture features of the 50% cut plane can better represent the macrotexture characteristics of the road surface.

Besides, by observing and comparing the NE values of each specimen under different conditions, it can be

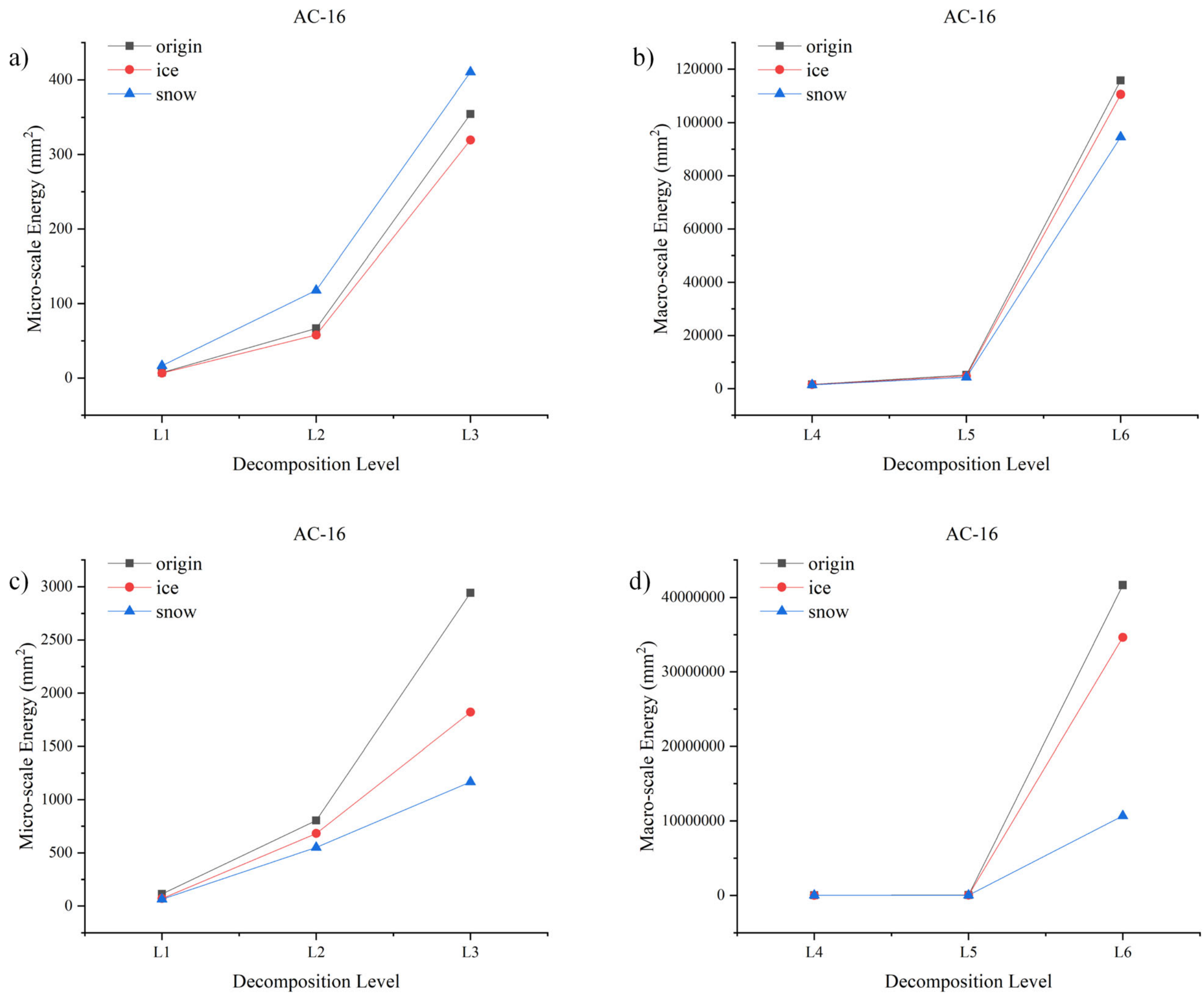

Fig. 9 The Energy Results of AC-16; **a** 50% Cutting Plane in micro-scale, **b** 50% Cutting Plane in macro-scale, **c** 100% Cutting Plane in micro-scale, **d** 100% Cutting Plane in macro-scale

found that, compared with the original surface, the NE value of the snowy surface decreases more than that of the icy surface. Only on the 50% cutting plane of AC-5 specimens, the NE value of the icy surface decreases more than that of the snowy surface, and the minimum value is 1.219. The reason why AC-5 had different results from others is when sprayed water on the surface, AC-5 formed an ice sheet on the surface because of its dense structure. At the same time, water sprayed on other specimens permeated into the texture slot and frozen. On the 100% cutting plane, the minimum value of NE is 160.525 measured by the snowy AC-5 specimen. It can be known that ice and snow will reduce the pavement surface macrotexture and the snow has a more significant impact on pavement texture than ice does.

Comparison between MTD and NE

A simple comparison between MTD and NE values was given in the previous section. The statistical correlation between MTD and NE for each specimen in different conditions was presented in Table 2. The correlation coefficient (R^2) is used to evaluate the correlation between the two parameters and distinguish the accuracy of their data. The results in this Table suggest that NE is directly related to MTD and can be described by a simple linear relationship (i.e., y = ax+b). It is evident that when a 50% cutting plane was chosen, the correlation between MTD and NE would show a higher R^2 value, which indicates that the texture upper than 50% height can almost represent the surface macrotexture.

In addition, Fig. 13 displays a comparison between MTD and NE on the 50% cutting plane for each

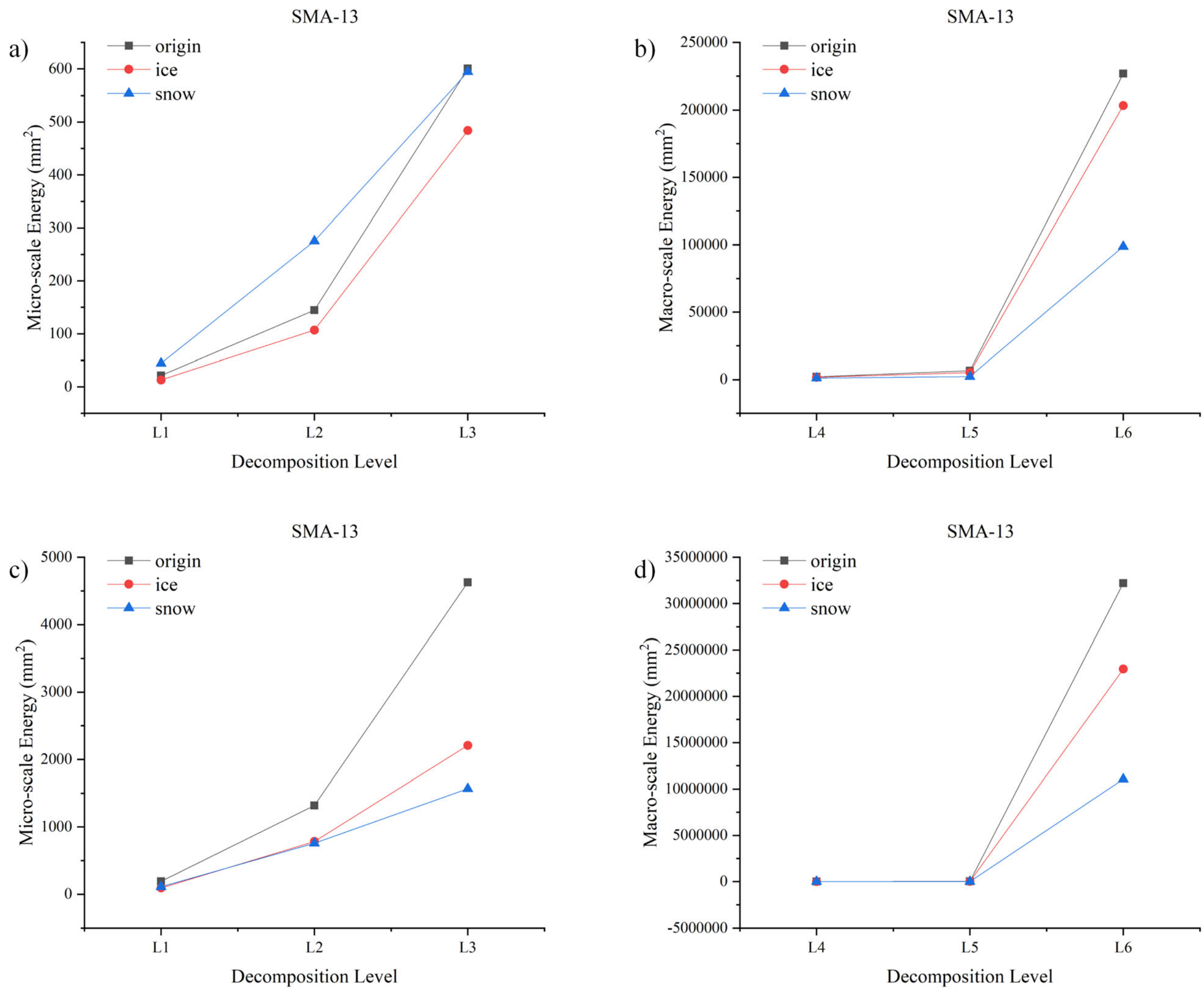

Fig. 10 The Energy Results of SMA-13; **a** 50% Cutting Plane in micro-scale, **b** 50% Cutting Plane in macro-scale, **c** 100% Cutting Plane in micro-scale, **d** 100% Cutting Plane in macro-scale

specimen in different conditions. For simplicity, the MTD values and the NE values were plotted on the same figure. The NE values were shown in the form of a histogram with the vertical axis on the left. The MTD values were shown in the form of a scatter diagram with the vertical axis on the right. For the convenience of observation, the three points under different conditions of the same gradation type were connected into three-point line segments.

It is shown in this figure that the trends (increase, decrease, or no change) in macrotexture properties among the specimens were consistent for both MTD and NE. However, compared with MTD values, the NE values have the advantages of full coverage, full automation and wide analytical scale. Firstly, the variations in the macrotexture properties are better captured using the NE than the MTD. The NE values are calculated based on the entire pavement texture information. In contrast, the MTD values use the sand patch method, a fixed-point detection method, to not reflect the macrotexture of the whole region. Out of the vehicle driving characteristics in daily life, the wheel tracks on the road surface are distributed on the cross-section of the lane according to certain rules, and they also have randomness. Therefore, the texture characteristics of the whole pavement surface should be analyzed, which shows that the NE value has practical value due to its full coverage advantage. Secondly, the use of the computer algorithm realizes the automatic measurement of pavement texture properties, this greatly reduces the tedious manual calculation. Thirdly, because of a high-resolution three-dimensional profile scanner and wavelet transform method, NE

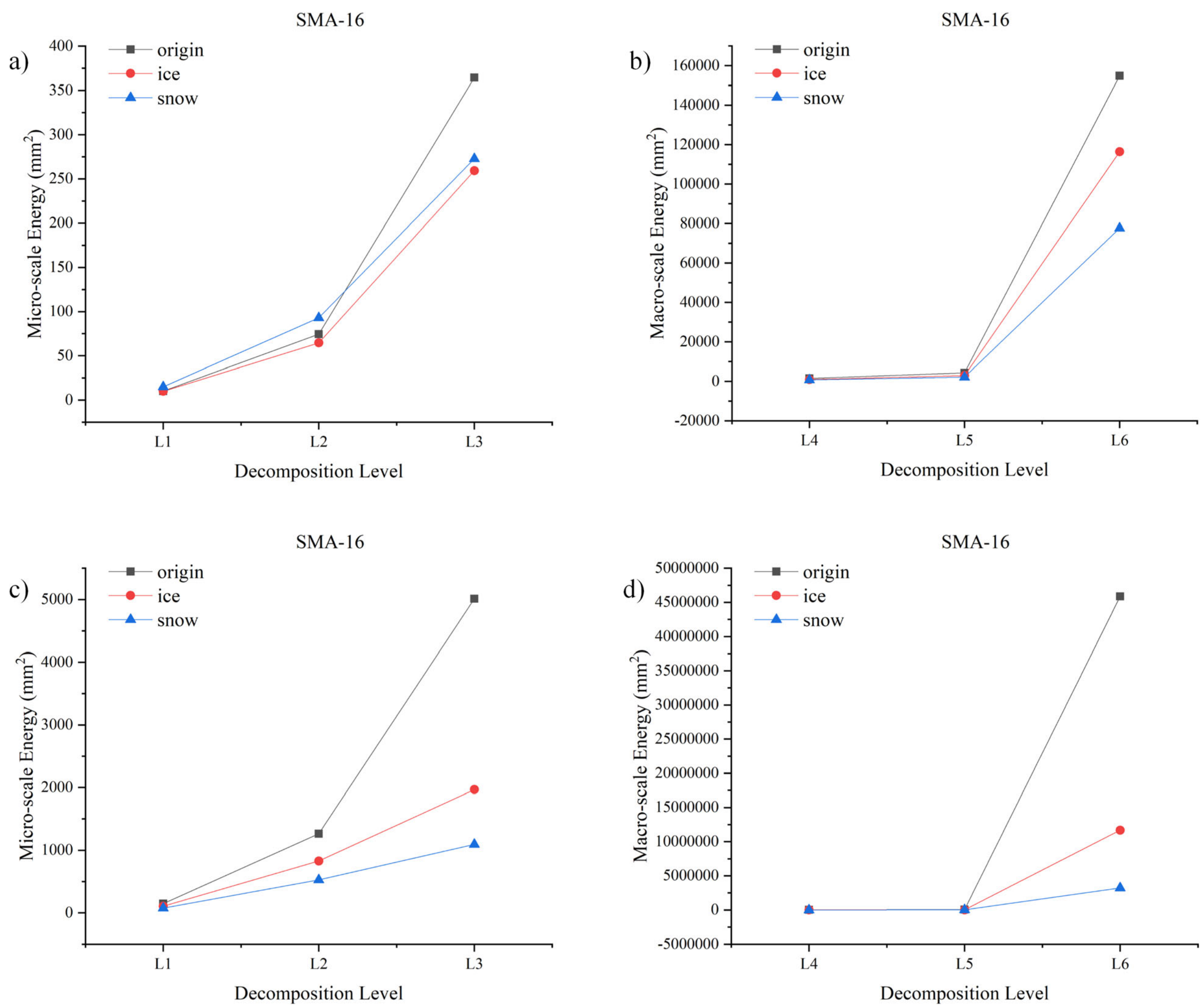

Fig. 11 The Energy Results of SMA-16; **a** 50% Cutting Plane in micro-scale, **b** 50% Cutting Plane in macro-scale, **c** 100% Cutting Plane in micro-scale, **d** 100% Cutting Plane in macro-scale

extracts and analyzes the pavement texture properties on micro and macro scales respectively, and the analysis scale was wider. Above all, it suggests that the wavelet approach is better suited to characterize the macrotexture properties of asphalt pavements.

Conclusions

In this study, a 2D-wavelet transform approach was proposed to decompose the 3D pavement texture measured by a high-resolution 3D profile scanner into micro-scale and macro-scale in two directions. The asphalt pavement specimens consisted of two asphalt mixture types (asphalt concrete (AC) and stone mastic asphalt (SMA)), and the pavement surface was under different conditions (original, icy, and snowy). The surface topography was made a top cut off at 50% and 100% height before decomposition. The Normalized Energy (NE) was used as the wavelet-based indicator. Through the observation and data analysis of the experimental results in this paper, the following conclusions were obtained:

(1) The 2D-wavelet transform approach can be used as a tool to make in-depth use of the high-resolution 3D data, and then the road performances, such as skid resistance and degree of wear, can be evaluated. It shows that the Normalized Energy (NE), a macro texture description index based on the 2D-wavelet approach proposed in this paper, has a strong correlation with the traditional index MTD. MTD and NE results show the same trend of macroscopic

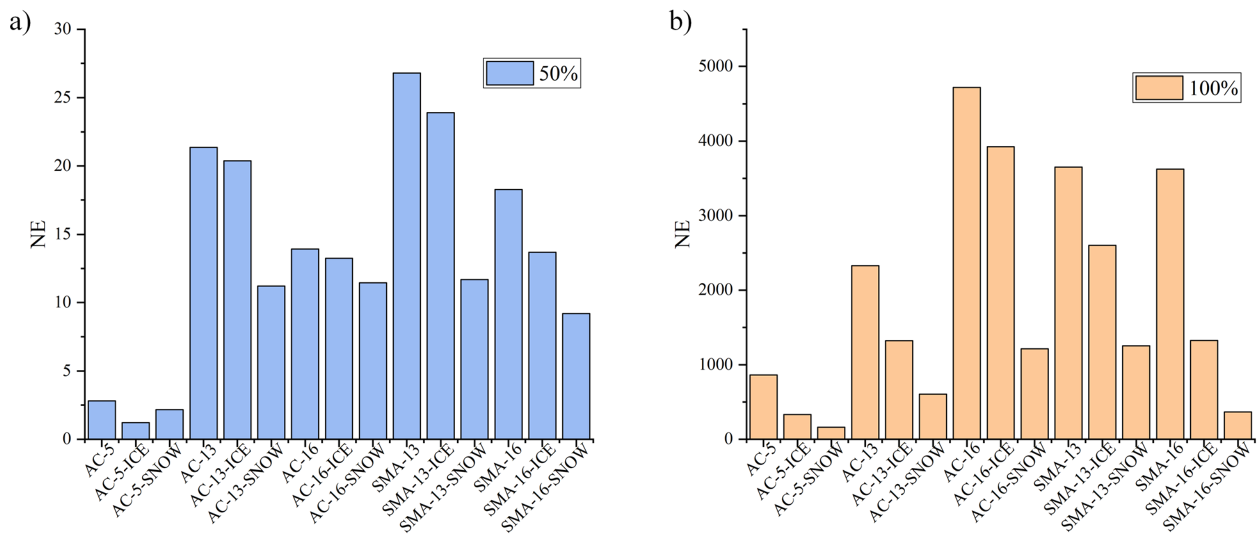

Fig. 12 The NE result; **a** The NE results on 50% cutting plane, **b** the NE results on 100% cutting plane

texture. Compared with MTD values, the NE values have the advantages of full coverage, full automation and wide analytical scale. Therefore, the 2D-wavelet transform approach is more suitable for the characterization of texture properties of pavement surfaces.

(2) The 2D-wavelet transform approach is further applied to analyze the texture properties on the pavement covered with snow and ice. On the micro-scale, original surfaces had the highest micro-scale energy, and icy surfaces had the lowest micro-scale energy. The snow increased the micro-scale texture of the pavement surface because of its fluffiness, which led to severe irregularities on the micro-scale, and the snowy surface had abundant micro-scale texture. The formation of the ice sheets on the surface reduced the micro-scale texture, making the texture of the icy surface the simplest. As for the macro scale, the origin surfaces had the highest energy, and the snowy surfaces had the lowest energy. The reason for this was that the filling effect of snow and ice on the surface reduced the macro-scale texture of the pavement surface.

(3) The 2D-wavelet transform approach can be used to extract and analyze the micro and macro texture, and can be applied to both scientific researches and engineering practice in a future study. For example, nowadays, the unmanned drive is a hot topic in today's smart city construction. This approach can be applied to improve the intelligent driving braking system due to its full automation characteristics, which can provide pavement texture feature information for the safe braking strategy of driverless vehicles and improve the braking safety of driverless vehicles.

Table 2 Correlation between MTD and NE

Cutting Plane	Condition	Equation	R^2
50%	Original	MTD = 0.045NE + 0.699	0.7616
	Icy	MTD = 0.045NE + 0.624	0.7146
	snowy	MTD = 0.079NE + 0.324	0.9489
100%	Original	MTD = 0.0003NE + 0.637	0.7153
	Icy	MTD = 0.0003NE + 0.791	0.5806
	snowy	MTD = 0.0006NE + 0.633	0.7466

Note: R^2 means the correlation coefficient

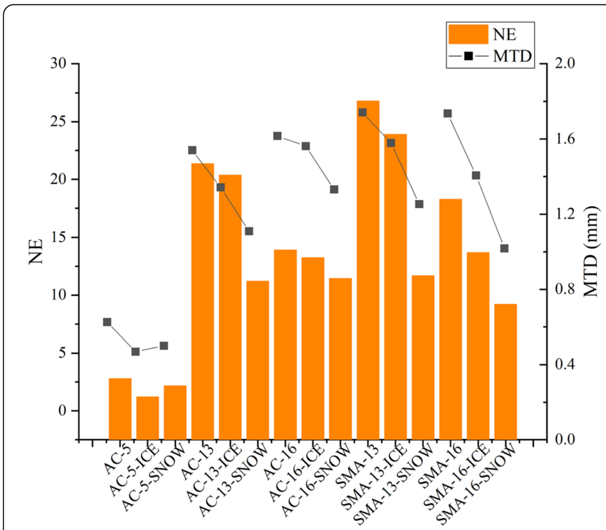

Fig. 13 Comparison between MTD and NE for 50% cutting plane

Finally, in a follow-up study, we will attempt to use long-term texture monitoring to evaluate the wavelet-energy variation during traffic loads adequately. Further research can focus on both the macro and micro-texture under different gradation types and working conditions.

Abbreviations
AC: Asphalt Concrete; DSM: Digital Surface Model; ITAM: Image-based Texture Analysis Method; MPD: Mean Profile Depth; MTD: Mean Texture Depth; NE: Normalized Energy; NMAS: Nominal Maximum Aggregate Size; PCC: Portland Cement Concrete; PIARC: Permanent International Association of Road Congress; PSD: Power Spectral Density; RE: Relative Energy; RMS: Root Mean Square; SMA: Stone Mastic Asphalt; SMTD: Sensor Measured Texture Depth

Acknowledgements
Not applicable.

Authors' contributions
FL and SZ participated in the design of this study, GA carried out the study and collected important backgroundinformation, ZW and YD provided assistance for data acquisition, data analysis and statistical analysis, GA and YL both drafted the manuscript. All authors read and approved the final manuscript.

Funding
This research was supported by the Department of Transportation of Shandong Province (No. 2018BZ4) and National Key R&D Program of China (2018YFB1600100).

Availability of data and materials
Not applicable.

Declarations

Competing interests
The authors declare that they have no competing interests.

Author details
[1]School of Transportation Science and Engineering, Beihang University, Beijing 100191, China. [2]Shandong Provincial Communications Planning and Design Institute CO., LTD, Jinan 250031, Shandong, China. [3]Key Laboratory of Road and Traffic Engineering of Ministry of Education, Tongji University, Shanghai 200092, China.

Received: 28 February 2021 Accepted: 14 April 2021
Published online: 07 May 2021

References

1. Abbas A, Kutay ME, Azari H, Rasmussen R (2007) Three-dimensional surface texture characterization of Portland cement concrete pavements. Comput Aided Civil Infrastruct Eng 22(3):197–209. https://doi.org/10.1111/j.1467-8667.2007.00479.x
2. Al-Rousan T, Masad E, Tutumluer E, Pan T (2007) Evaluation of image analysis techniques for quantifying aggregate shape characteristics. Constr Build Mater 21(5):978–990. https://doi.org/10.1016/j.conbuildmat.2006.03.005
3. Andreas U, Dawei WM, Oeser BS (2015) Calculation of skid resistance from texture measurements. J Traf Transact Eng 2(1):3–16
4. Ayenu-Prah AY, Attoh-Okine NO (2009) Comparative study of Hilbert-Huang transform, Fourier transform, and wavelet transform in pavement profile analysis. Veh Syst Dyn 47(4):437–456. https://doi.org/10.1080/00423110802167466
5. Huang B, Tian W, Li J, Cui EF (2008) Method for quantitative evaluation of skid resistance of asphalt pavement. China J Highway Transport (Chinese Edition) (04):12–17
6. Cafiso S, Taormina S (2007) Texture analysis of aggregates for wearing courses in asphalt pavements. Int J Pavement Eng 8(1):45–54. https://doi.org/10.1080/10298430600898307
7. De C, Nima R, S., Hussain B. (2015) Exploring the feasibility of evaluating asphalt pavement surface macro-texture using image-based texture analysis method. Road Mat Pavem Des 16(2):405–420
8. De C (2020) Evaluating asphalt pavement surface texture using 3D digital imaging. Int J Pavement Eng 21(12)416–427
9. Du Y, Weng Z, Li F, Ablat G, Liu C (2020) A novel approach for pavement texture characterisation using 2d-wavelet decomposition. Int J Pavement Eng 6:1–16
10. El GA, Shalaby A, Saleh M, Flintsch G (2011) Stereo-vision applications to reconstruct the 3D texture of pavement surface. Int J Pavement Eng 12(3): 263–273
11. Hu L, Yun D, Liu Z, Du S, Zhang Z, Bao Y (2016) Effect of three-dimensional macrotexture characteristics on dynamic frictional coefficient of asphalt pavement surface. Constr Build Mater 126:720–729. https://doi.org/10.1016/j.conbuildmat.2016.09.088
12. Chen H, Wu Y, Xia H, Jing B, Zhang Q (2018) Review of ice-pavement adhesion study and development of hydrophobic surface in pavement deicing. J Traf Transpor Eng 5(3):224–238. https://doi.org/10.1016/j.jtte.2018.03.002
13. Kanafi MM, Tuononen AJ (2017) Top topography surface roughness power spectrum for pavement friction evaluation. Tribol Int 107:240–249. https://doi.org/10.1016/j.triboint.2016.11.038
14. Kogbara RB, Masad EA, Kassem E et al (2016) A state-of-the-art review of parameters influencing measurement and modeling of skid resistance of asphalt pavements, 2016. Constr Build Mater 114(1):602–617
15. Li S, Harris D, Wells T (2016) Surface texture and friction characteristics of diamond-ground concrete and asphalt pavements. J Traf Transpor Eng 3(5): 475–482
16. Mistakidis ES, Panagouli OK, Panagiotopoulos PD (1998) Unilateral contact problems with fractal geometry and fractal friction laws: methods of calculation. Comput Mech 21(4–5):353–362. https://doi.org/10.1007/s004660050312
17. Sharifi NP, Chen S, You Z, van Dam T, Gilbertson C (2019) A review on the best practices in concrete pavement design and materials in wet-freeze climates similar to Michigan. J Traf Transpor Eng 6(3):245–255. https://doi.org/10.1016/j.jtte.2018.12.003
18. Persson BNJ (2001) Theory of rubber friction, contact mechanics and the role of surface roughness on the adhesion of elastic solids. 160th meeting of the rubber division, American Chemical Society, Cleveland
19. PIARC (1987) Report of the committee on surface characteristics. permanent International Association of Road Congress (PIARC) XVIII world road congress, Brussels
20. Puzzo L, Loprencipe G, Tozzo C, D'Andrea A (2017) Three-dimensional survey method of pavement texture using photographic equipment. Measurement 111:146–157. https://doi.org/10.1016/j.measurement.2017.07.040
21. Qiang JL, Zhan Y, Yang G et al (2018) Pavement skid resistance as a function of pavement surface and aggregate texture properties. Int J Pavement Eng 21(2):1–11
22. Reginald B, Kogbara E, Masad A, David W, Phillip M (2018) Relating surface texture parameters from close range photogrammetry to grip-tester pavement friction measurements. Construct Building Mat 166:227–240
23. Wang D, Chen X, Yin C, Oeser M, Steinauer B (2013) Influence of different polishing conditions on the skid resistance development of asphalt surface. Wear 308(s1–s2):71–78
24. Wang D, Ueckermann A, Schacht A, Oeser M, Steinauer B, Persson BNJ (2014) Tire–road contact stiffness. Tribol Lett 56(2):397–402. https://doi.org/10.1007/s11249-014-0417-x
25. Wang Y, Yang Z, Liu Y, Sun L (2018) The characterisation of three-dimensional texture morphology of pavement for describing pavement sliding resistance. Road Mat Pavem Des 2018:1–20
26. Xin Q, Qian Z, Miao Y, Meng L, Wang L (2017) Three-dimensional characterization of asphalt pavement macrotexture using laser scanner and microelement. Road Mat Pavem Des 18(sup3):190–199
27. Yang G, Li QJ, Zhan YJ, Wang KCP, Wang C (2017) Wavelet based macrotexture analysis for pavement friction prediction. KSCE J Civ Eng 22(2018);117–124
28. Khan ZH, Islam MR, Tarefder RA (2019) Determining asphalt surface temperature using weather parameters. J Traf Transpor Eng 6(6):577–588. https://doi.org/10.1016/j.jtte.2018.04.005
29. Zelelew H, Khasawneh M, Abbas A (2014) Wavelet-based characterization of asphalt pavement surface macro-texture. Road Mat Pavem Des 15(3):622–641. https://doi.org/10.1080/14680629.2014.908137

30. Zelelew HM, Papagiannakis AT, Izeppi EDD (2013) Pavement macro-texture analysis using wavelets. Int J Pavement Eng 14(8):725–735. https://doi.org/10.1080/10298436.2012.705004
31. Zhang X, Liu T, Liu C, Chen Z (2014) Research on skid resistance of asphalt pavement based on three-dimensional laser-scanning technology and pressure-sensitive film. Constr Build Mater 69:49–59. https://doi.org/10.1016/j.conbuildmat.2014.07.015

Publisher's Note

Springer Nature remains neutral with regard to jurisdictional claims in published maps and institutional affiliations.